# CUT&RUN reveals unique positioning of pre-initiated RNA polymerase II in the steady state of transcription

Michi Miura* and Honglin Chen

State Key Laboratory for Emerging Infectious Diseases and

Department of Microbiology, The University of Hong Kong,

Hong Kong SAR, China

*Email: michi.miura.res@gmail.com

## Abstract

CUT&RUN is a powerful tool to study protein-DNA interactions *in vivo*. DNA fragments cleaved by the targeted micrococcal nuclease identify the footprints of DNA-binding proteins on the chromatin. We performed CUT&RUN on human lung carcinoma cell line A549 maintained in a multi-well cell culture plate to profile RNA polymerase II. Size-fractionation of aligned reads revealed that the collection of long (>270 bp) DNA fragments corresponded to the bimodal peak around the transcription start sites, as previously seen with chromatin immunoprecipitation. However, we found that shorter (<120 bp) fragments identify a well-defined peak localised at the transcription start sites. This distinct DNA footprint of shorter fragments, which constituted only about 5% of the total reads, indicates the unique positioning of the poised RNA polymerase II before transcription initiation, which has not been detected in the steady state of transcription by standard chromatin immunoprecipitation.



**Keywords:** CUT&RUN; protein-DNA interaction; RNA polymerase II; transcription initiation; promoter-proximal pausing; chromatin profiling

38 # Introduction

39 CUT&RUN (Cleavage Under Targets and Release Using Nuclease) (Skene & Henikoff,
40 2017) is a powerful tool to map protein-DNA interactions *in vivo*. CUT&RUN directs
41 Protein A/G-fused micrococcal nuclease (pAG-MNase) (Meers, Bryson, Henikoff, &
42 Henikoff, 2019) to the antibody-bound protein-DNA complex, with a subsequent release
43 of the DNA fragments cleaved in the presence of calcium ions. There are two major
44 advantages of CUT&RUN over conventional chromatin immunoprecipitation (ChIP).
45 First, CUT&RUN does not require sonication for chromatin fragmentation. Physical
46 shearing of chromatin by sonication does not occur randomly, which can skew signal
47 detection; and excessive sonication may attenuate the epitope of the target protein
48 (Marx, 2019). Second, CUT&RUN identifies the footprints of DNA-binding proteins on
49 the chromatin, which revealed distinct binding configurations of transcription factors in
50 yeast (Skene & Henikoff, 2017) and mammalian cells (Meers, Janssens, & Henikoff,
51 2019).

52 In this study, we performed CUT&RUN on the human lung carcinoma cell line A549
53 maintained in a multi-well cell culture plate (Figure 1A) to profile RNA polymerase II (Pol
54 II) around the transcription start sites (TSS). We found that CUT&RUN could validate
55 the bimodal signal around the TSS as previously detected using ChIP (Erickson,
56 Sheridan, Cortazar, & Bentley, 2018). However, we also identified a distinct peak at the
57 TSS from short DNA fragments released only by pAG-MNase. This finding indicates a
58 transient positioning of the pre-initiated RNA polymerase II in the steady state of
59 transcription, which has eluded detection by conventional ChIP (Erickson et al., 2018).

60

61

62 # Results

63 **Overall performance of "CUT&RUN on plate" for profiling Pol II**

64 First, we tested the feasibility of performing CUT&RUN on adherent cells attached to a
65 multi-well polystyrene cell culture plate with Pol II antibodies (Figure 1A). Pol II signals
66 obtained by this method are shown in Figure 1B. The genomic region chr6 p22.2 was
67 selected due to the presence of multiple histone genes. This location is ideal for efficient
68 visual inspection of Pol II signals because of the compact size and close spacing of these
69 genes. Our Pol II signals consistently mapped to the transcription units of histone genes
70 with low background as previously reported (Meers, Bryson, et al., 2019; Skene &
71 Henikoff, 2017) (Figure 1B). The signals along the gene body, in addition to 1.5 kb
72 upstream of the TSS and downstream of the transcription end site (TES), were averaged
73 over "singletons" (genes that are separated from other genes by >2 kb) (Figure 1C),
74 showing consistent enrichment around the TSS. Therefore, through the successful
75 capture of Pol II signals *in situ* with low background, the performance of our "CUT&RUN
76 on plate" (or CROP) protocol was shown to be comparable with the conventional
77 CUT&RUN (Meers, Bryson, et al., 2019; Skene & Henikoff, 2017).

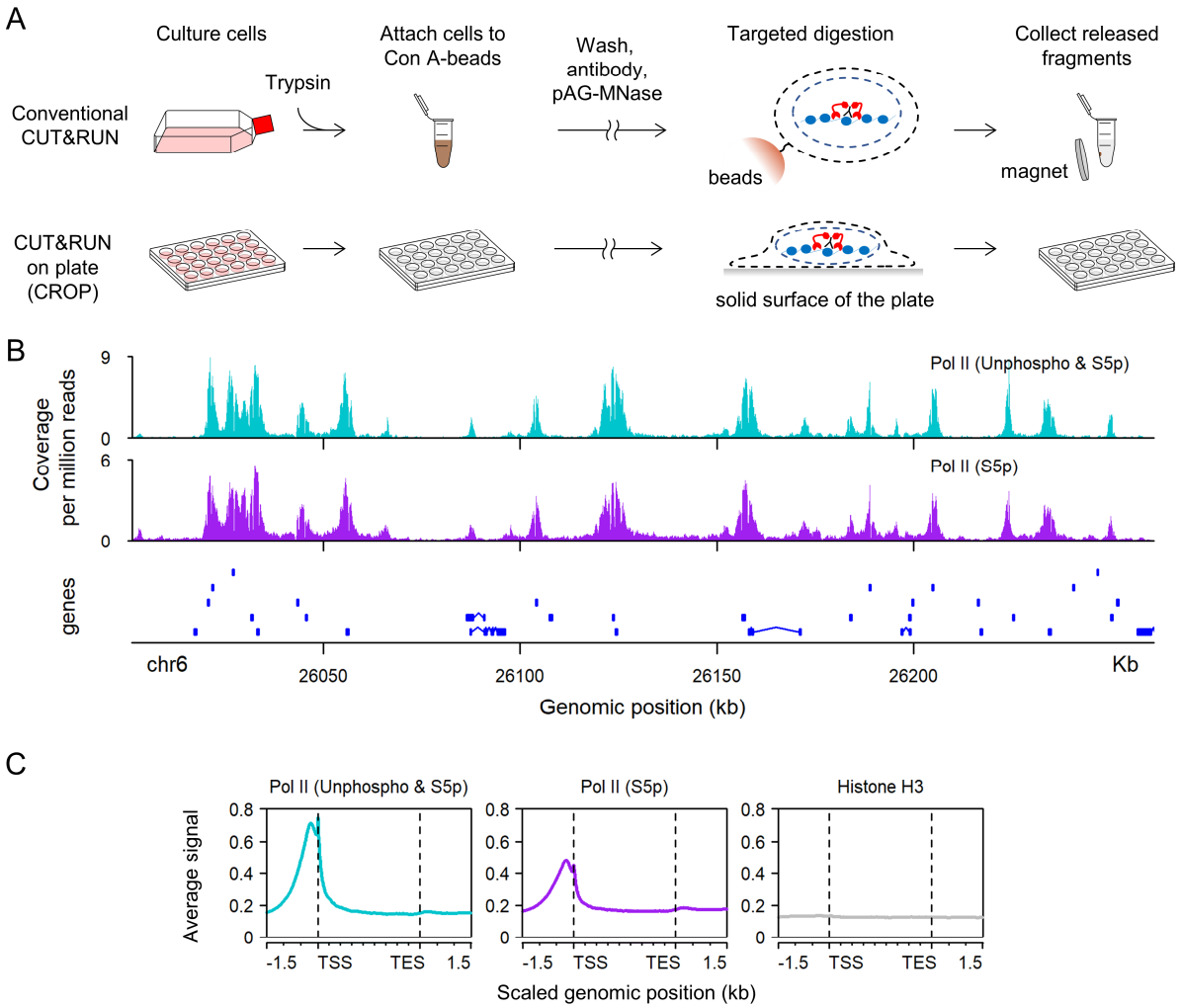


## Figure 1 Overall performance of "CUT&RUN on plate"

(A) Protocol overview. In conventional CUT&RUN (top row), cells are harvested and attached on Concanavalin A-magnetic beads. Subsequent cell permeabilisation, antibody binding, and targeted pAG-MNase digestion are performed on these cells immobilised on the beads. The magnetic beads are captured each time the buffers are changed. "CUT&RUN on plate" (or CROP) (bottom row) circumvents the use of Concanavalin A-magnetic beads. Adherent cells are anchored on the solid surface of the multi-well plate throughout the protocol, enabling rapid buffer change for multiple samples. (B) Pol II signals in the histone gene cluster obtained by CROP. The Pol II signal is expressed by the coverage normalised with the total read count. (C) Metaplot analysis of the Pol II signal. Pol II signal was averaged over genes that are at least 2 kb away from other genes. The region between 1.5 kb upstream of the transcription start site (TSS) and 1.5 kb downstream of the transcription end site (TES) is presented. The length of the gene body is scaled to 3 kb.

92 **Size-fractionation of aligned reads to reveal distinct footprints of Pol II-binding**

93 The size distribution of aligned paired-end reads showed multiple peaks (Figure 2A). We
94 categorised the aligned reads into 5 subsets by length (Figure 2A), each of which is
95 expected to reflect a unique footprint of the protein-DNA interaction (Meers, Janssens,
96 et al., 2019; Skene & Henikoff, 2017). The size of DNA fractions was shown to reveal
97 distinct signals of Pol II around the TSS (Figure 2B). The signal of the total reads (i.e.
98 without size-fractionation) conformed to the characteristic bimodal peak as previously
99 reported by ChIP (i.e. the peaks located at either ~150 bp upstream or downstream of
100 the TSS) (Erickson et al., 2018). By contrast, the shorter fragments (<120 bp)
101 constituted a single narrow peak at the TSS, and the longer fragments (>120 bp)
102 accumulated adjacent to the TSS (Figure 2B). As expected, the bimodal signal of the
103 longer fragments (>270 bp) is skewed towards the region downstream of the TSS (Figure
104 2B) (Erickson et al., 2018). To validate our findings, we analysed the TSS of individual
105 genes. We confirmed that some genes showed an accumulation of longer (>270 bp)
106 fragments on both sides of the TSS (Figure 2C), whereas some other genes had signals
107 on only one side (Figure 2D and E). The signals of the shorter (<120 bp) and longer
108 (>270 bp) fragments were mutually exclusive, showing two distinct footprints of Pol II
109 adjacent to each other. The shorter fragments constituted only about 5% of the total
110 reads (Figure 2A).

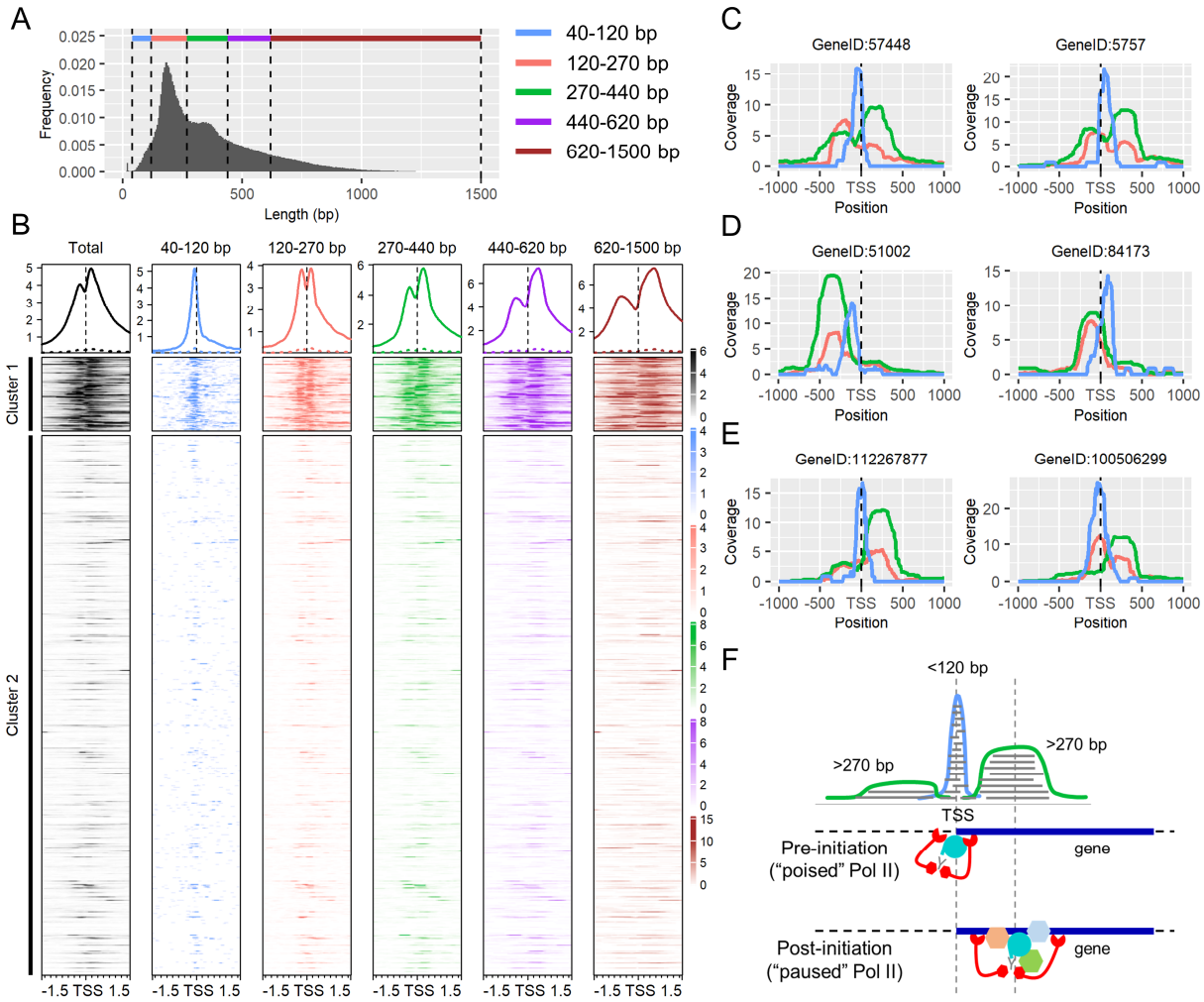


**Figure 2 Size-fractionation identifies distinct Pol II footprints**

(A) Size distribution of aligned reads (the insert size between the sequence adaptors). The reads were categorised into five subsets by size, each of which is coded by a unique colour. (B) Pol II signal (Millipore, 05-623; unphosphorylated and S5p) from each size fraction in ±1.5 kb around the transcription start site (TSS). The signals in 13,452 annotated RefSeq singleton genes are presented in the heatmap; a *k*-mean clustering was performed on the total reads (coded in black) to enrich genes with Pol II signal (Cluster 1 and Cluster 2). The metaplot for each cluster is shown above the heatmap (Cluster 1, solid line; Cluster 2, dashed line). (C-E) Pol II signal (Millipore, 05-623; unphosphorylated and S5p) in ±1 kb around the transcription start site of individual genes. The vertical axis indicates the pile-up of aligned reads from the three size fractions. The same colour codes are used as per panel (A). Note that the coverage was normalised per million reads within each of the size fractions; the relative coverage within each plot is not proportional to the actual occurrence of these fractions. (F) A schematic drawing of the Pol II footprints deduced by the alignment of size-fractionated reads.

126 Recent studies using ChIP-seq, as well as nascent transcript sequencing, have shown
127 that Pol II is paused at ~50 bp downstream of the TSS (Core, Waterfall, & Lis, 2008;
128 Erickson et al., 2018; Kwak, Fuda, Core, & Lis, 2013; Nojima et al., 2015; Shao &
129 Zeitlinger, 2017). Our observations suggest two distinct binding configurations of Pol II
130 near the TSS (Figure 2F). These configurations are: (1) poised Pol II at the TSS in the
131 pre-initiation state where nucleosomes are depleted, and (2) paused Pol II upstream or
132 downstream of the TSS where Pol II pausing is regulated by a higher-molecular complex
133 after transcription initiation. The paused Pol II peaks were visible exclusively in the
134 longer (>120 bp) fragments adjacent to the TSS. We reason that this is because Pol II
135 is associated with a higher-molecular complex at the paused site (Vos, Farnung, Urlaub,
136 & Cramer, 2018), which protects the chromatin from the pAG-MNase cleavage. As a
137 result, pAG-MNase is unable to produce shorter (<120 bp) fragments associated with
138 the paused Pol II. Composite signals were observed in our assay (Figure 2C to E), each
139 of which corresponds to one of the two distinct binding configurations as described.
140 These composite signals result from CUT&RUN taking a 'snapshot' of each gene from
141 hundreds of thousands of cells per assay at the TSS; a transcription start site
142 accommodates one molecule of Pol II at a time, either at the TSS (pre-initiation) or the
143 site of promoter-proximal pausing (post-initiation) (Gressel et al., 2017; Shao &
144 Zeitlinger, 2017).

145

146 **Impact of formaldehyde fixation on "CUT&RUN on plate"**

147 Formaldehyde fixation is often used to investigate transient protein interactions. We
148 tested if formaldehyde fixation can be implemented in "CUT&RUN on plate". Cells were
149 fixed with 1.5% formaldehyde in either pre- or post-cellular permeabilisation (see

150 Materials and Methods). Although formaldehyde fixation reduced the detection of Pol II

151 signals, serine 5-phosphorylated (S5p) Pol II was shown to be enriched near the TSS

152 (Figure 3A).

153

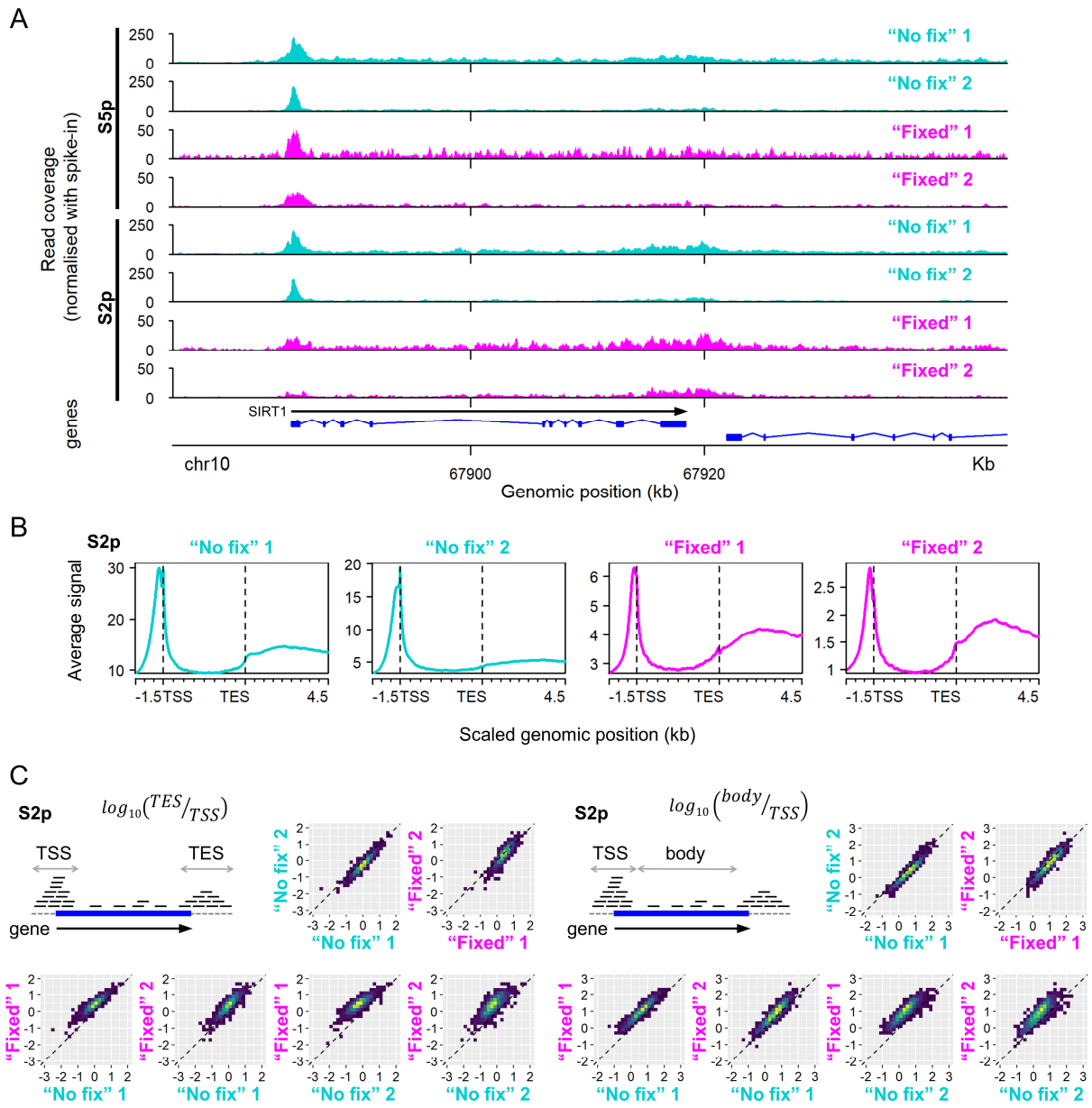


154

155 **Figure 3 Impact of formaldehyde cell fixation on the S2p Pol II signals**

156 (A) S5p and S2p Pol II signal over a gene on chr10 (SIRT1) (S5p, ab5131; S2p, ab5095). Two colour codes
157 indicate whether cells were fixed with formaldehyde (cyan, "No fix"; magenta, "Fixed"). Cells were fixed
158 following a brief cytoplasmic extraction ("Fixed" 1) or intact cells were fixed directly ("Fixed" 2). The signals
159 were normalised with the yeast spike-in DNA. (B) Metaplot analyses of S2p Pol II signal from 1.5 kb
160 upstream of the transcription start site (TSS) to 4.5 kb downstream of the transcription end site (TES). The
161 signals were averaged over the singleton genes (n = 13,452). The gene body is scaled to 4.5 kb in length.
162 (C) Two Pol II metrics measuring the ratio of signals in the gene body to TSS (left) and in the TES to TSS
163 (right). These metrics were calculated for genes (n = 1,435) that were longer than 5 kb and aggregated in
164 Cluster 1 (Figure 2B). The metrics of each gene are plotted for each combination of the assays and the
165 density of plots are represented by colour brightness (navy to yellow). The data is presented in the
166 logarithmic scale (base = 10) for ease of visualisation.

167

168 We observed a profound effect of formaldehyde fixation on the serine 2-phosphorylated
169 (S2p) Pol II signal (Figure 3A). The metaplot analysis showed that the average signal of
170 S2p RNA polymerase II over the singleton genes was more pronounced in the region
171 downstream of the TES when cells were fixed (Figure 3B). This observation was
172 confirmed by signal quantification in the gene body or TES (relative to that in the TSS
173 respectively), for each singleton gene (Figure 3C, schematic drawing). While these
174 metrics for each gene were in good concordance within the same fixation condition, we
175 found that the ratio of S2p Pol II signal in the gene body to TSS, or in the TES to TSS
176 was higher when the cells were fixed (Figure 3C, "No Fix" vs "Fixed"). We consider two
177 possible explanations of this observation: (1) fixation stabilises the elongating S2p RNA
178 polymerase II on the DNA, or more likely, (2) fixation preferentially reduces the detection
179 of Pol II near the TSS, thereby altering the ratio of signals in the TSS, gene body and
180 TES.

181

182

183

184 **Discussion**

185 In this study, we have devised "CUT&RUN on plate" (CROP) for profiling protein-DNA
186 interactions in adherent cells maintained in a multi-well cell culture plate. The current
187 CUT&RUN protocol (Hainer & Fazzio, 2019; Meers, Bryson, et al., 2019; Skene, Henikoff,
188 & Henikoff, 2018) relies on Concanavalin A-coated magnetic beads to immobilise the
189 cells before the targeted pAG-MNase cleavage. This immobilisation step introduces a
190 range of shortcomings associated with the use of Concanavalin A-beads. For example,
191 trypsinisation while harvesting the cells may alter the behaviour of DNA-binding
192 proteins and lower the binding affinity of cells to Concanavalin A. Concanavalin A also
193 stimulates certain types of cells. When the plasma membrane is removed to investigate
194 the nuclei, Concanavalin A does not bind efficiently to the nuclear membrane. Finally,
195 Concanavalin A-beads tend to aggregate when cells are attached. Our CROP protocol
196 described here overcomes these key problems associated with the use of Concanavalin-
197 A beads and may find widespread application.

198 Using CUT&RUN, we profiled RNA polymerase II near the transcription start sites. The
199 turnover of Pol II near the TSS is highly dynamic (Darzacq et al., 2007; Erickson et al.,
200 2018; Steurer et al., 2018). Since the duration of Pol II in the promoter-proximal
201 pausing state is about ten times longer than that of Pol II in the pre-initiation state
202 (Darzacq et al., 2007; Steurer et al., 2018), a majority of reads obtained by either ChIP
203 or CUT&RUN is from the paused site, approximately 50 bp downstream of the TSS.
204 Because ChIP fragments are typically hundreds of base pairs long, the rare signal of the
205 poised Pol II at the TSS is often obscured. While Erickson *et al.* had previously identified
206 the signal of the poised Pol II at the TSS by ChIP, this signal was only exposed following
207 the depletion of Pol II in hypotonic condition with the use of triptolide to block the

208 initiation (Erickson et al., 2018). Nascent transcript sequencing is, by its nature, unable
209 to capture the poised RNA polymerase II before transcription initiation. In contrast, we
210 accurately identified the positioning of poised Pol II in the physiological condition
211 through the recovery of its unique footprint (Figure 2F). Therefore, CUT&RUN is an
212 effective substitute for the conventional chromatin immunoprecipitation to investigate
213 the behaviour of RNA polymerase II at promoters.

214 # Materials and Methods

215 **Cells**

216 Human lung carcinoma cell line A549 was maintained in Dulbecco's Modified Eagle
217 Medium (Gibco, 11965-092) supplemented with 10% FBS (Gibco, 16140-071), 100 U/ml
218 penicillin and 100 μg/ml streptomycin (Gibco, 15140-122).

219

220 **CUT&RUN in a cell culture plate**

221 CUT&RUN was performed on a standard 24-well cell culture plate (TPP, 92012); cells
222 were left attached to the bottom of the well throughout the protocol.

223 A549 was seeded in wells and grown to ~70 to 90% confluency (~0.5 million cells) at the
224 time of an assay. Cells were washed with PBS and permeabilised with Perm buffer (0.1%
225 Triton X-100 (Sigma, X100), 20 mM HEPES-KOH pH 7.5, 150 mM NaCl, 0.5 mM
226 Spermidine (Sigma, S2626) and proteinase inhibitor (Roche, 04 693 132 001)) for 15
227 min at room temperature. After removing Perm buffer, cells were washed again with
228 Perm buffer and incubated with an antibody (~0.7 μg) in 150 μl Perm buffer per well for
229 one hour at room temperature. The antibodies used in this study were: mouse anti-
230 RNA polymerase II (Millipore, 05-623; clone CTD4H8; 0.75 μg per well); rabbit anti-RNA
231 polymerase II (phospho S2) (Abcam, ab5095; polyclonal; 0.75 μg per well); and rabbit
232 anti-RNA polymerase II (phospho S5) (Abcam, ab5131; polyclonal; 0.675 μg per well).
233 After incubation, unbound antibody was removed, and cells were washed twice with
234 Perm buffer. Cells were then incubated with the recombinant pAG-MNase (Cell
235 Signaling, 40366; 1:33 volume) in 150 μl Perm buffer per well for an hour at room
236 temperature. Unbound pAG-MNase was removed, and cells were washed twice with

237 Perm buffer. During the second wash of this stage, the plate was placed on ice-cold
238 water. For pAG-MNase activation, 150 µl ice-cold Perm buffer containing 5 mM $CaCl_2$
239 was dispensed per well, and the plate was incubated on ice-cold water for 30 min. The
240 pAG-MNase digestion was halted by the addition of 50 µl 4× STOP solution (680 mM
241 NaCl, 40 mM EDTA (Sigma, E5134), 8mM EGTA (AG Scientific, E-2491), 100 µg/ml
242 RNase A (Invitrogen, 12091021) and 0.1% Triton X-100). The plate was incubated at
243 37°C for 30 min to facilitate the release of digested DNA fragments from the nucleus.
244 The supernatant was collected, and DNA was extracted using DNeasy Blood & Tissue
245 Kit (Qiagen, 69504).

246 In addition to the native "CUT&RUN on plate" described above, two protocols for cell
247 fixation with 1.5% formaldehyde were tested: (1) cells were fixed with 1.5% formaldehyde
248 for 10 min prior to the cell permeabilisation with Perm buffer; and (2) cells were fixed
249 following the permeabilisation (5 min in Perm buffer). The supernatant collected at the
250 end of the CUT&RUN protocol was supplemented with 1% SDS (final concentration) and
251 incubated at 65°C overnight for de-crosslinking. The DNA was purified with QIAquick
252 PCR Purification Kit (Qiagen, 28104).

253

254 **Pair-end sequencing and read alignment**

255 DNA libraries were constructed using NEBNext Ultra II DNA Library Prep Kit for Illumina
256 (NEB, E7645) with index primers (NEB, E7335 and E7710). Fragmented genomic DNA
257 from *S. cerevisiae* (Cell Signaling, 40366) was used (10 pg per sample) as spike-in.

258 DNA libraries were sequenced (150 bp × 2) with NovaSeq 6000 (Illumina), and the initial
259 50 bases of each read were aligned to a concatenation of human reference genome
260 (GRCh38) and *S. cerevisiae* (sacCer3) with a BWA algorithm (version 0.7.17) `bwa mem`

261 (Li & Durbin, 2009). Duplications of reads were marked with a Picard tool (version
262 2.18.9) `MarkDuplicates` (http://broadinstitute.github.io/picard). Only a minority of
263 the aligned reads (less than 0.151%) constituted the yeast genome, thereby confirming
264 the successful recovery of DNA fragments cleaved by pAG-MNase. A subset of aligned
265 reads was selected for the downstream analyses using Samtools (version 1.9) with the
266 following commands: SAM flag 3 (read paired; read mapped in proper pair) (`samtools`
267 `view -f 3`); mapping quality greater than 20 (`samtools view -q 20`); without tags
268 `'XA:Z:'` and `'SA:Z:'` (`grep -v -e 'XA:Z:' -e 'SA:Z:'`); and aligned in either one of
269 the chromosomes chr1 to chr22, chrX or chrY (`samtools view chr1 chr2 ... chrY`).

270

271 **Data analyses and visualisation**

272 Aligned reads were fractionated by size (the 9th field of SAM) and stored in the BAM
273 format. Read coverage was computed and stored in the bigWig format with deepTools's
274 (version 3.1.3) `bamCoverage` (Ramirez et al., 2016), normalised per million reads. For
275 comparison of the Pol II signals across the fixation conditions (Figure 3A and B), read
276 coverage was computed with deepTools's (version 3.3.2) `bamCoverage` using scale
277 factors calculated with the number of spike-in reads mapped to the yeast genome. The
278 bigWig files were converted into the bedGraph format using `bigWigToBedGraph` (UCSC)
279 and the read coverage was visualised with the R package Sushi (version 1.24.0)
280 (Phanstiel, Boyle, Araya, & Snyder, 2014) in R (version 3.6.2). A matrix containing the
281 read coverage over a given region of genes was computed using deepTools's (version
282 3.3.2) `computeMatrix` with an annotation
283 GCA_000001405.15_GRCh38_full_analysis_set.refseq_annotation (NCBI). A subset of
284 genes that were separated from other genes by >2 kb was considered for this analysis;

285 such genes were extracted using bedtools's (version 2.26.0) (Quinlan & Hall, 2010)
286 `merge` and `intersect`. The matrix was visualised as a heatmap and a metaplot using
287 the R package EnrichedHeatmap (version 1.16.0) (Gu, Eils, Schlesner, & Ishaque, 2018).

288

289 **Signal quantification in the TSS, gene body and TES**

290 The regions for TSS, gene body and TES were defined: TSS, ±0.5 kb around the start
291 site of a gene; gene body, from 0.5 kb downstream of the start site to 1.5 kb upstream
292 of the end site; and TES, 1.5 kb upstream of the end site to 4.5 kb downstream of the
293 end site. For each of the TSS, gene body and TES regions, genome coordinates for the
294 singleton genes in the RefSeq annotation were stored in the BED format.

295 The BAM files containing the aligned paired reads were converted into the BED format
296 with bedtools's `bamtobed -bedpe` and the subsequent extraction of the 1st
297 (chromosome), 2nd, 6th (the start and end positions of an alignment, respectively), 7th,
298 8th and 9th fields.

299 For each singleton gene, paired reads aligned to the TSS, gene body or TES were counted
300 using bedtools's `intersect -F 0.5` (reads that overlapped by less than half of the
301 alignment length were rejected). The read counts in the gene body and TES were
302 normalised with the number of reads contained in the TSS.

## Acknowledgements

We thank Liew Jun Mun at University of Cambridge, for reviewing the manuscript to enhance the readability. We also thank Prof. Charles R. M. Bangham at Imperial College London, for reviewing the manuscript and critical comments. Illumina NovaSeq 6000 sequencing was performed at Centre for PanorOmic Sciences (CPOS) Genomics Core, LKS Faculty of Medicine, The University of Hong Kong. This study was supported in part by the Research Grants Council of the Hong Kong SAR (17119618, 17107019 and C7027-16G).

## Competing interests

The authors declare no competing interests.

314 **References**


315 Core, L. J., Waterfall, J. J., & Lis, J. T. (2008). Nascent RNA sequencing reveals
316 widespread pausing and divergent initiation at human promoters. *Science,*
317 *322*(5909), 1845-1848. doi:10.1126/science.1162228

318 Darzacq, X., Shav-Tal, Y., de Turris, V., Brody, Y., Shenoy, S. M., Phair, R. D., & Singer,
319 R. H. (2007). In vivo dynamics of RNA polymerase II transcription. *Nat Struct Mol*
320 *Biol, 14*(9), 796-806. doi:10.1038/nsmb1280

321 Erickson, B., Sheridan, R. M., Cortazar, M., & Bentley, D. L. (2018). Dynamic turnover
322 of paused Pol II complexes at human promoters. *Genes Dev, 32*(17-18), 1215-
323 1225. doi:10.1101/gad.316810.118

324 Gressel, S., Schwalb, B., Decker, T. M., Qin, W., Leonhardt, H., Eick, D., & Cramer, P.
325 (2017). CDK9-dependent RNA polymerase II pausing controls transcription
326 initiation. *Elife, 6*. doi:10.7554/eLife.29736

327 Gu, Z., Eils, R., Schlesner, M., & Ishaque, N. (2018). EnrichedHeatmap: an
328 R/Bioconductor package for comprehensive visualization of genomic signal
329 associations. *BMC Genomics, 19*(1), 234. doi:10.1186/s12864-018-4625-x

330 Hainer, S. J., & Fazzio, T. G. (2019). High-Resolution Chromatin Profiling Using
331 CUT&RUN. *Curr Protoc Mol Biol, 126*(1), e85. doi:10.1002/cpmb.85

332 Kwak, H., Fuda, N. J., Core, L. J., & Lis, J. T. (2013). Precise maps of RNA polymerase
333 reveal how promoters direct initiation and pausing. *Science, 339*(6122), 950-953.
334 doi:10.1126/science.1229386

335 Li, H., & Durbin, R. (2009). Fast and accurate short read alignment with Burrows-
336 Wheeler transform. *Bioinformatics, 25*(14), 1754-1760.
337 doi:10.1093/bioinformatics/btp324

338 Marx, V. (2019). What to do about those immunoprecipitation blues. *Nat Methods, 16*(4),
339 289-292. doi:10.1038/s41592-019-0365-3
340 Meers, M. P., Bryson, T. D., Henikoff, J. G., & Henikoff, S. (2019). Improved CUT&RUN
341 chromatin profiling tools. *Elife, 8*. doi:10.7554/eLife.46314
342 Meers, M. P., Janssens, D. H., & Henikoff, S. (2019). Pioneer Factor-Nucleosome Binding
343 Events during Differentiation Are Motif Encoded. *Mol Cell, 75*(3), 562-575 e565.
344 doi:10.1016/j.molcel.2019.05.025
345 Nojima, T., Gomes, T., Grosso, A. R. F., Kimura, H., Dye, M. J., Dhir, S., . . . Proudfoot,
346 N. J. (2015). Mammalian NET-Seq Reveals Genome-wide Nascent Transcription
347 Coupled to RNA Processing. *Cell, 161*(3), 526-540.
348 doi:10.1016/j.cell.2015.03.027
349 Phanstiel, D. H., Boyle, A. P., Araya, C. L., & Snyder, M. P. (2014). Sushi.R: flexible,
350 quantitative and integrative genomic visualizations for publication-quality multi-
351 panel figures. *Bioinformatics, 30*(19), 2808-2810.
352 doi:10.1093/bioinformatics/btu379
353 Quinlan, A. R., & Hall, I. M. (2010). BEDTools: a flexible suite of utilities for comparing
354 genomic features. *Bioinformatics, 26*(6), 841-842.
355 doi:10.1093/bioinformatics/btq033
356 Ramirez, F., Ryan, D. P., Gruning, B., Bhardwaj, V., Kilpert, F., Richter, A. S., . . .
357 Manke, T. (2016). deepTools2: a next generation web server for deep-sequencing
358 data analysis. *Nucleic Acids Res, 44*(W1), W160-165. doi:10.1093/nar/gkw257
359 Shao, W., & Zeitlinger, J. (2017). Paused RNA polymerase II inhibits new transcriptional
360 initiation. *Nat Genet, 49*(7), 1045-1051. doi:10.1038/ng.3867

361 Skene, P. J., Henikoff, J. G., & Henikoff, S. (2018). Targeted in situ genome-wide
362 profiling with high efficiency for low cell numbers. *Nat Protoc, 13*(5), 1006-1019.
363 doi:10.1038/nprot.2018.015
364 Skene, P. J., & Henikoff, S. (2017). An efficient targeted nuclease strategy for high-
365 resolution mapping of DNA binding sites. *Elife, 6*. doi:10.7554/eLife.21856
366 Steurer, B., Janssens, R. C., Geverts, B., Geijer, M. E., Wienholz, F., Theil, A. F., . . .
367 Marteijn, J. A. (2018). Live-cell analysis of endogenous GFP-RPB1 uncovers rapid
368 turnover of initiating and promoter-paused RNA Polymerase II. *Proc Natl Acad Sci*
369 *U S A, 115*(19), E4368-E4376. doi:10.1073/pnas.1717920115
370 Vos, S. M., Farnung, L., Urlaub, H., & Cramer, P. (2018). Structure of paused
371 transcription complex Pol II-DSIF-NELF. *Nature, 560*(7720), 601-606.
372 doi:10.1038/s41586-018-0442-2

373